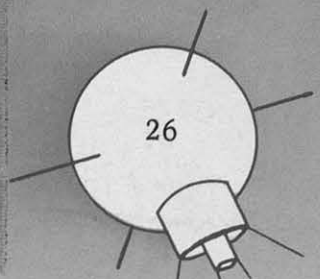


*MESOMETEOROLOGY PROJECT*

*Department of the Geophysical Sciences*
*The University of Chicago*

# AN EXPERIMENT IN THE DETERMINATION OF GEOSTROPHIC AND ISALLOBARIC WINDS FROM NSSP PRESSURE DATA

by

William Bonner

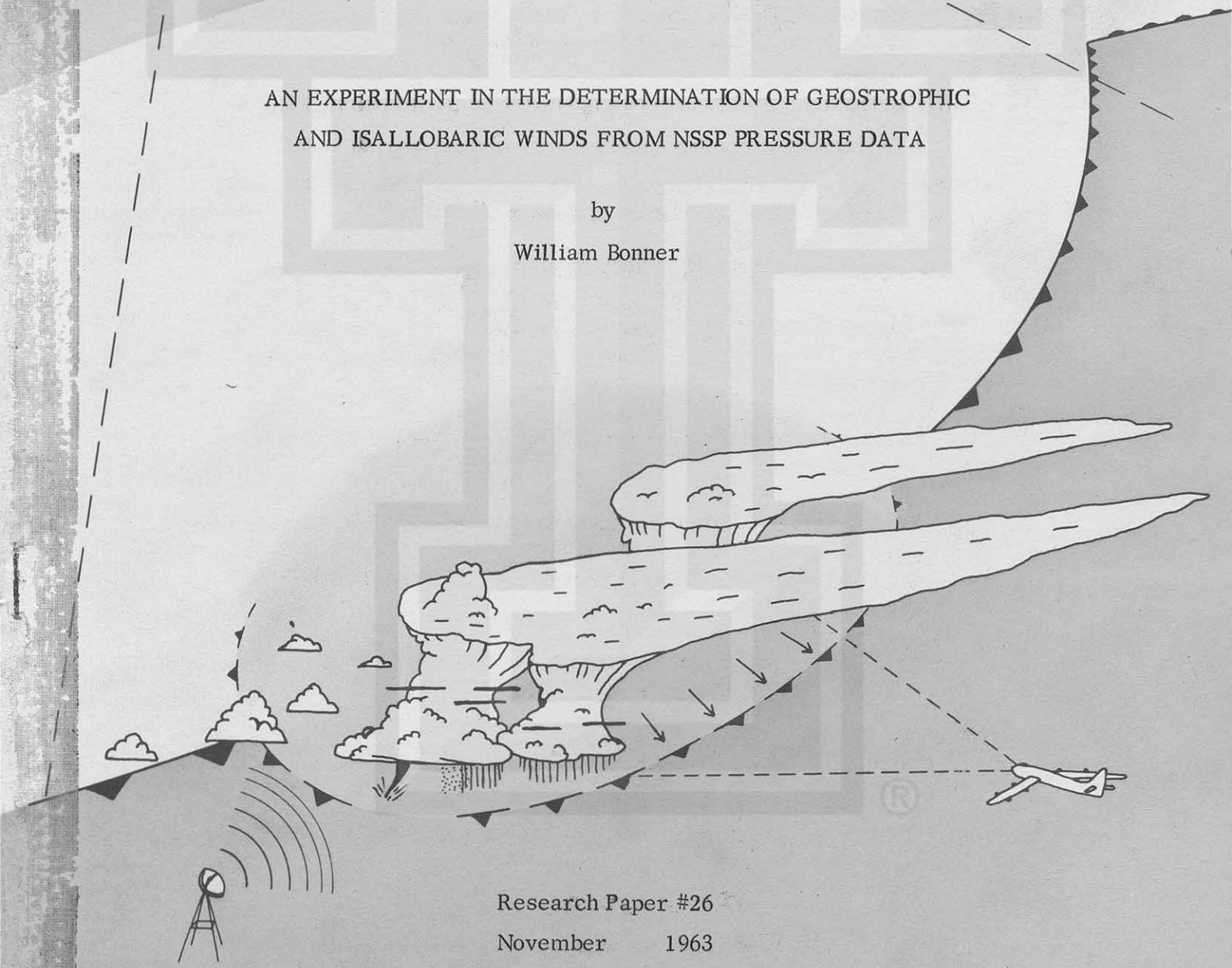

Research Paper #26

November 1963

MESOMETEOROLOGY PROJECT --------RESEARCH PAPERS

1. Report on the Chicago Tornado of March 4, 1961 - Rodger A. Brown and Tetsuya Fujita *
2. Index to the NSSP Surface Network - Tetsuya Fujita *
3. Outline of a Technique for Precise Rectification of Satellite Cloud Photographs - Tetsuya Fujita *
4. Horizontal Structure of Mountain Winds - Henry A. Brown *
5. An Investigation of Developmental Processes of the Wake Depression Through Excess Pressure Analysis of Nocturnal Showers - Joseph L. Goldman *
6. Precipitation in the 1960 Flagstaff Mesometeorological Network - Kenneth A. Styber *
7. On a Method of Single- and Dual-Image Photogrammetry of Panoramic Aerial Photographs - Tetsuya Fujita (To be published)
8. A Review of Researches on Analytical Mesometeorology - Tetsuya Fujita
9. Meteorological Interpretations of Convective Nephsystems Appearing in TIROS Cloud Photographs - Tetsuya Fujita, Toshimitsu Ushijima, William A. Hass, and George T. Dellert, Jr.
10. Study of the Development of Prefrontal Squall-Systems Using NSSP Network Data - Joseph L. Goldman
11. Analysis of Selected Aircraft Data from NSSP Operation, 1962 - Tetsuya Fujita
12. Study of a Long Condensation Trail Photographed by TIROS I - Toshimitsu Ushijima
13. A Technique for Precise Analysis of Satellite Data; Volume 1 - Photogrammetry - (Published as MSL Report No. 14) - Tetsuya Fujita
14. Investigation of a Summer Jet Stream Using TIROS and Aerological Data - Kozo Ninomiya
15. Outline of a Theory and Examples for Precise Analysis of Satellite Radiation Data - Tetsuya Fujita

* Out of Print

(Continued on back cover)

MESOMETEOROLOGY PROJECT

Department of the Geophysical Sciences

The University of Chicago

# AN EXPERIMENT IN THE DETERMINATION OF GEOSTROPHIC AND ISALLOBARIC WINDS FROM NSSP PRESSURE DATA

by

William Bonner

RESEARCH PAPER #26

The research reported in this paper has been sponsored by the National Severe Storms Project, United States Weather Bureau, under grant CWB WBG-8.

Table of Contents

## ABSTRACT

Geostrophic and isallobaric winds are computed in the vicinity of a low-level jet stream. Pressure and pressure tendency fields are determined by analysis of microbarograph traces from NSSP stations. Wind speeds in the jet are found to be super-geostrophic during the day as well as at night. The night-time increase in speed takes place roughly as described by Blackadar (1957). The isallobaric winds do not contribute in any organized fashion to the wind speeds in the jet and inclusion of the isallobaric term gives a worse estimate of the actual wind than does the simple geostrophic approximation.

## 1. Introduction

Pressure, temperature and humidity traces from the cooperative stations maintained by the National Severe Storms Project have provided, to a large extent, the observational basis for the development of models of mesoscale disturbances over the Great Plains (see Fujita, 1962). The use of such data, however, is not restricted to the study of severe storms. The 210 stations of the NSSP alpha network (Fig. 1) cover an area large enough to be useful in the study of some synoptic-scale features as well.

This report is a continuation of an earlier study (Bonner, 1963) involving the relationship between the low-level jet stream and thunderstorm activity during a particular twenty-four hour period. The same case is examined again; this time, with the emphasis upon the kinematics of the low-level jet stream and, in particular, upon the determination of geostrophic and isallobaric winds in the vicinity of the low-level jet.

Estimation of geostrophic winds from standard pressure analysis in this region is difficult for several reasons:

1. The high station elevations and strongly sloping terrain introduce large errors into the estimation of the horizontal pressure gradient from the gradient of sea-level pressures (Sangster, 1959; Fujita, 1962).
2. The distance between standard synoptic stations is too large to allow for completely independent analyses of wind and pressure fields.

3. The low-level jet stream is typically found in connection with widespread thunderstorm activity (Pitchford and London, 1962); it is difficult if not impossible to define the synoptic-scale features of the pressure fields without first performing a fairly detailed mesoanalysis.

By using the NSSP pressure data, reduced in the manner developed by Fujita and Brown (1957), and described by Fujita (1962), it is possible to at least minimize the errors arising from each of the factors listed above.

The study was begun as a test of an hypothesis about the low-level jet stream. Wexler (1961) has stated that the jet, in the south-central United States, cannot be described purely as a diurnal oscillation of the wind — that the large-scale features of the flow must be considered as well. In a case study presented by Newton (1956), a strong low-level jet is observed to the south-east of a cyclone moving across the Great Plains. It seemed possible that, in such a case, the isallobaric winds in the vicinity of the cyclone could contribute significantly to the wind speeds in the jet — leading, perhaps, to supergeostrophic winds during the daytime and increasing the ageostrophic component of the flow at night — and that this might be an important factor in producing a strong, three-dimensional southerly jet.

As a preliminary test of this hypothesis, a statistical study was made of the extent to which strong jet observations are restricted to the night-time hours and of the synoptic conditions under which they occur. Isallobaric winds were then computed in the vicinity of a low-level jet stream. While the case chosen was far from ideal — the pressure center was relatively weak and located on the northern boundary of the NSSP area — the pressure traces had been calibrated and much of the work involved in identifying the individual mesosystems had been performed in connection with the earlier study.

## 2. The Statistical Study

Vertical wind soundings published in the Northern Hemisphere Data Tabulations were examined for the period, October, 1959, through September, 1960. A low-level jet observation was defined in the following way:

> The wind speed must reach a relative maximum within the first 1.5 km above the ground and decrease by at least 3 m sec $^{-1}$ to the next higher minimum or to the 3 km level, whichever is lower.

Similar definitions have been used by Blackadar (1957) and Pitchford and London (see Means, 1962). All wind maxima satisfying this criterion were recorded; however, data are presented only for pronounced wind maxima — where the wind speed at the level of maximum wind and the decrease above are greater than or equal to 16 m sec $^{-1}$ and 8 m sec $^{-1}$ respectively. While the selection of these figures is arbitrary, the percentages of low-level jet observations occurring at each observation time were found to be relatively insensitive to the particular values chosen.

Diurnal variations in the frequency of occurrence of strong jet maxima near the ground are summarized in Table 1. Wind maxima at both stations are clearly much more common at night than during the day. However, they are not entirely a night-time phenomenon. For instance, in Table 1, more than one out of every four jet observations at Topeka, Kansas occurred on the daytime soundings. While this does not dispute Blackadar's explanation or description of the nocturnal jet (Blackadar, 1957), it does indicate that processes other than the purely frictional or radiative effects may be important (Wexler, 1961).

Daily weather maps published by the U.S. Weather Bureau were examined on each of the days with strong southerly[1] jets on the midnight observation. On roughly 60 percent of the "jet days" at each station, cold fronts or low pressure centers were to be found within 350 n mi to the west of the station. On roughly one-half of these days, frontal passage occurred within the next twelve hours. Thus, while a moving low or frontal system is certainly not essential to the formation of a low-level jet, there appears to be enough of an association to justify an examination of the contribution of the isallobaric wind to the wind speeds in the jet.

---

1 Data in Table 1 refers to all jet observations regardless of the wind direction at the level of maximum wind. More than 70 percent of these jets, however are classified as southerly ( wind directions from 135 to 255 deg).

Table 1. Diurnal Variations in the Frequency of occurrence of strong low-level wind maxima at Fort Worth, Texas and Topeka, Kansas — October, 1959 through September 1960. Column A gives the number of jet observations; Column B, the percentage of the total jet observations occurring at each observation time.

| OBSERVATION | FORT WORTH | | TOPEKA | |
|---|---|---|---|---|
| TIME | A | B | A | B |
| 18 CST | 8 | 7.8 | 18 | 16.2 |
| 00 CST | 36 | 35.0 | 47 | 42.3 |
| 06 CST | 46 | 44.7 | 33 | 29.7 |
| 12 CST | 13 | 12.5 | 13 | 11.8 |
| Total | 103 | 100.0 | 111 | 100.0 |

3. Calculation of the Isallobaric Wind

The isallobaric component of the wind,

$$\vec{V}_{is} = -\frac{\alpha}{f^2} \nabla \frac{\partial p}{\partial t} \qquad (1)$$

(Petterssen, 1956) was computed from the gradient of pressure tendencies as determined from microbarograph traces at Weather Bureau, FAA and cooperative stations within the general region of the NSSP network (Fig. 1). During the period chosen, thunderstorm activity was widespread in this area and pressure traces were highly disturbed by the mesoscale systems. Therefore, the first step in computing an isallobaric wind that was representative of the large scale flow was the elimination of the mesoscale disturbances from the individual pressure traces.

Small scale variations in pressure of the order of minutes were simply smoothed out of the traces. In the vicinity of recognizeable mesosystems, smoothed pressure traces were obtained by connecting the undisturbed traces at beginning and end of the "disturbed" period and then plotting a series of hourly smoothed pressure maps based upon this first estimate of the undisturbed

pressure. The traces at individual stations were then adjusted to give a pattern of undisturbed pressures that was regular and consistent in both space and time.

While the errors in the pressure tendencies at any given station are estimated to be as large as 0.5 mb per 2 hrs simply from the inaccuracies in reading the charts due to alignment problems, thickness of the ink line and errors in the tracing of the original records, the tendency fields are actually overdetermined. The station density is much greater than would be required in order to determine the broad-scale features of the tendency fields and smoothed isallobars could be drawn by subjectively averaging the tendencies at a number of stations within a very small area.

Before proceeding with the discussion of the isallobaric wind, several features of the pressure traces in the vicinity of squall lines will be mentioned.

The boundary of a typical mesoscale disturbance associated with a squall line is generally drawn to coincide with the leading edge of the pressure surge line (see Fujita, 1962). In most of the cases examined here, it was necessary to consider the disturbed area of the pressure trace as extending well ahead of the pressure jump. A pressure drop was typically observed ahead of an advancing mesohigh. This drop, in several cases, was very pronounced and could not possibly be considered to be a "normal" feature of the pressure field. The most distinct pressure fall of this type occurred ahead of a well-organized squall line moving through the northern boundary of the NSSP area. Pressure traces and smoothed pressure fields in the vicinity of this squall line are shown in Figs. 2 through 5. A similar fall is apparent in pressure traces in northwest Texas during the formation of a squall line in this area (Fig. 6). The pressure traces in Fig. 6 give the appearance of a thunderstorm high embedded within a mesolow (see also Fig. 19). In northern Kansas, however, the low appears to form ahead of and possibly as the result of the squall line itself.

The pressure drop, in other cases, was very weak but still evident from the calculation of pressure tendencies. For instance, the pressure trace at Kalvesta, Kansas (not shown) indicated only a slight increase in the rate at which the pressure was falling, beginning about 40 minutes before the passage of a strong

pressure surge line. At this time, the pressure tendency increased from an average rate of approximately 1.5 mb per 2 hrs to an instantaneous rate of 3.5 mb per 2 hrs — too large to be explained by the synoptic-scale features of the flow.

Pressure and pressure tendency fields at each of the standard wind observation times are shown in Figs. 7 through 11. The gradient of $\partial p/\partial t$ in the vicinity of the low at 06 CST and 12 CST gives an excellent estimation of the movement of the cyclone from the Petterssen kinematic expression (Petterssen 1956); the instantaneous pressure tendency at the center of the low at the same observations times (with the diurnal tendency removed) gives the average observed rate of filling of the low. Thus, the configuration and the size of the pressure tendencies at these times are essentially representative of the behavior of the synoptic-scale cyclone. The small region of pressure falls ahead of the advancing cold front (Fig. 9) appears to be an almost sub-synoptic feature of the type mentioned earlier in connection with pressure surge lines. Since the tendencies, however, are of an appropriate magnitude for synoptic-scale disturbances, this pressure dip was retained in the analysis.

Geostrophic and isallobaric components of the wind were computed at the intersections of latitude and longitude lines separated by 1.5 deg within the region of southerly flow. Geostrophic winds, isallobaric winds, and observed winds at 1 km above the ground are shown vectorially in Figs. 12 through 16.

The isallobaric components of the wind are quite large in a number of cases — of the order of 10 to 15 m sec $^{-1}$. They do not, however, contribute in any organized fashion to the wind speeds in the vicinity of the low-level jet. For instance, at 12 CST, 16 May (Fig. 12), a narrow zone of wind speeds greater than or equal to 20 m sec $^{-1}$ is located in western Kansas. Most of this zone is to the north of the center of pressure falls (Fig. 7) and the isallobaric component of the wind is contributing in exactly the opposite sense to that expected.

Wind speeds at 00 CST (Fig. 14) are now greater than 20 m sec $^{-1}$ throughout almost the entire area. The jet appears as a center of maximum winds — wind speeds approaching 30 m sec $^{-1}$ — located in Kansas and Oklahoma. Along 36 deg N, there is a component of the isallobaric wind in the direction of the ob-

served wind; further south, however, the contribution of the isallobaric wind is negative. At 37.5 deg N, nearly uniform wind speeds are observed at neighboring points where the isallobaric components are large and nearly 180 deg out of phase. In general, the hypothesis of an organized contribution to the wind speeds in the jet, arising from the isallobaric wind, is completely rejected by the data.

Not only does the isallobaric wind fail to contribute in an organized fashion to the jet, it fails to give, in most cases, an approximation to the actual wind that is as good as the simple geostrophic assumption. Table 2 shows the vector error in the approximation of the wind at grid points first, by the geostrophic wind, and second, by the geostrophic wind modified by the isallobaric term. At each of the observation times, the mean value of the error vector is larger when the isallobaric wind is considered, suggesting that the concept of the isallobaric wind, advanced by Brunt and Douglas (1928), does not result in a useful approximation to the actual wind. The same conclusion has been reached by Haurwitz (1946) and by Houghton and Austin (1946) in studies of the winds at 10,000 feet.

Table 2. Error in the approximation of the observed winds at 1000m above the ground by the geostrophic wind, $\mathbb{V}_g$, and by the sum of geostrophic and isallobaric winds, $\mathbb{V}_g + \mathbb{V}_{is}$. Values shown are mean values of the vector error at grid points in the region of southerly flow. Units: m sec $^{-1}$

| Time Period | $\overline{\lvert \mathbb{V}-\mathbb{V}_g \rvert}$ | $\overline{\lvert \mathbb{V}-(\mathbb{V}_g+\mathbb{V}_{is}) \rvert}$ | Number of Grid Points |
|---|---|---|---|
| 12 CST | 4.9 | 6.2 | 30 |
| 18 CST | 7.6 | 9.5 | 33 |
| 00 CST | 9.6 | 11.8 | 23 |
| 06 CST | 8.9 | 9.2 | 19 |
| 12 CST | 4.7 | 8.3 | 17 |
| All Times | 7.1 | 8.9 | 122 |

A second test of the reality of the isallobaric wind was made by using the observed changes in the geostrophic and observed winds to examine the

validity of a fundamental approximation in the derivation of the isallobaric wind.

The complete expression (neglecting friction) for the horizontal wind may be written in the following way: (Haltiner and Martin, 1957)

$$\mathbb{V} = \overset{(1)}{\mathbb{V}_g} + \frac{1}{f}\mathbf{k} \times \overset{(2)}{\frac{\partial \mathbb{V}}{\partial t}} + \overset{(3)}{\frac{1}{f}\mathbf{k} \times \mathbb{V} \cdot \nabla \mathbb{V}} + \overset{(4)}{\frac{w}{f}\mathbf{k} \times \frac{\partial \mathbb{V}}{\partial z}} \quad . \qquad (2)$$

Inclusion of the isallobaric wind is an attempt to improve the geostrophic approximation (term 1, equation 2) by including the local acceleration of the wind. The local acceleration of the wind is then approximated by the local acceleration of the geostrophic wind. It can be shown that this approximation is not valid during the particular period chosen.

Table 3. Six-hour time changes in observed and geostrophic winds. Values are in m sec $^{-1}$ per 6 hrs and represent the average scalar magnitude of the acceleration vectors at grid points in the region of southerly flow. Error in the approximation is indicated by the mean magnitude of the difference between observed and geostrophic changes — roughly, the acceleration of the ageostrophic wind.

| Time Period | $\overline{\lvert\Delta\mathbb{V}\rvert}$ | $\overline{\lvert\Delta\mathbb{V}_g\rvert}$ | $\overline{\lvert\Delta\mathbb{V}-\Delta\mathbb{V}_g\rvert}$ | Number of Grid Points |
|---|---|---|---|---|
| 12 CST - 18 CST | 4.2 | 6.4 | 7.5 | 31 |
| 18 CST - 00 CST | 11.1 | 7.8 | 10.1 | 26 |
| 00 CST - 06 CST | 8.6 | 7.8 | 7.6 | 19 |
| 06 CST - 12 CST | 8.0 | 4.6 | 7.0 | 18 |
| All Times | 7.7 | 6.7 | 7.6 | 94 |

Table 3 shows the mean values of the 6-hr vector changes in observed and geostrophic winds. Mean values were computed from the values at individual grid points within the region of southerly flow. The mean value of the error in this approximation is of the same order of magnitude as the change in the wind vector itself. Thus, on the average, $\partial \mathbb{V}_g / \partial t$ was useless as an approximation to the observed changes in the wind. Neglecting the time rate of change of the thermal wind in the layer from the ground to 1000 m

above the ground, the error vectors are the time rate of change of the ageostrophic wind $\partial \mathbb{V}'/\partial t$ . During three of the four periods considered, the magnitude of this vector, on the average, is larger than the magnitude of $\partial \mathbb{V}_g/\partial t$ .

## 4. Geostrophic and Observed Winds

Detailed description of the jet proved to be impossible because of the lack of an adequate network of upper air stations to tie in with the surface analyses. However, a general discussion of the structure of the jet and of the time changes in the winds near the ground will be given, emphasizing those features that are relevant to Blackadar's explanation of the low-level jet (see Blackadar, 1957).

Cross-sections through the low level jet stream at 18 CST and 06 CST (Figs. 17 and 18) show a strong increase in the southerly flow during the night-time hours. The jet stream, incohesive at 18 CST, is apparent on the 06 CST section as a well defined center of maximum winds between Oklahoma City and Tulsa. A cross-section along this line could not be constructed at 00 CST since Oklahoma City did not report at this time and the report at Tulsa was complete only to approximately 1 km above the ground. However, the low-level jet stream appeared to be most pronounced at midnight on wind charts constructed at constant levels above the ground (see Fig. 14). Referring to Figs. 12 through 16, the zone of maximum winds at each of the observation times was generally unreflected in the geostrophic wind fields.

Fig. 19 shows the six-hour vector change in the wind at 1 km above the ground during the period from 18 CST to 00 CST. The acceleration of the wind is remarkably uniform over the entire region of southerly flow. Between 06 CST and 12 CST, the vector changes in the wind are again quite uniform within the region of southerly flow; however, the acceleration is in almost exactly the opposite sense (Fig. 20).

Vertical profiles of the observed and geostrophic winds at 18 CST and 06 CST at Tulsa, Oklahoma City and Fort Worth, Texas are shown in Fig. 21. Geostrophic winds above the level of the terrain were computed by analyzing mean virtual temperature fields in 50-mb increments from ground level to 700 mb. The

thermal wind equation (see, for instance, Haltiner and Martin, 1957) was then used to compute the geostrophic wind fields at successive pressure levels.

At 06 CST, all three stations show a distinct, super-geostrophic maximum in wind speed within the lowest 1.5 km above the ground. At the level of maximum wind, observed wind speeds at each station exceed the geostrophic speeds by 10 to 12 m $sec^{-1}$. The ageostrophic wind vector at all stations is directed to the left of the observed wind. If the only process acting were the inertial oscillation of a frictionally produced ageostrophic wind as proposed by Blackadar, the ageostrophic wind should be directed to the right of the motion at this time, indicating a local deceleration of the wind.

Schematic temperature profiles are included in Fig. 21 at Oklahoma City and Fort Worth, Texas. At Fort Worth, the level of maximum wind coincides almost exactly with an inversion surface. At Oklahoma City; however, no such correspondence is found. A general check of the wind and temperature soundings available from stations in the region of southerly flow revealed no consistent relationship between the wind maximum and an inversion surface. The correspondence at Fort Worth appeared to be the exception rather than the rule.

At 18 CST wind speeds at Tulsa and Fort Worth in the zone from 0.5 to 1.5 km above the ground are approximately geostrophic. The only station with a distinct supergeostrophic maximum in the vertical wind speed profile is Oklahoma City (see also Fig. 17). Winds at all levels, at each station are directed to the left of the geostrophic wind indicating a consistent acceleration of the air as it moves northward.

The higher level jet stream at 18 CST (Fig. 17) is apparent at all three stations in Fig. 21 as a super-geostrophic wind maximum near 2.5 km. No explanation of this phenomenon is attempted. This feature, and the northerly jet in the cold air near Amarillo at 06 CST (Fig. 18) indicate, however, that fairly strong wind maxima may occur at various levels in the atmosphere, with northerly or southerly flow. The southerly low-level jet can be regarded as a true phenomenon only in a statistical sense — as a well-organized feature that occurs with relatively high frequency at certain altitudes and in certain regions.

Comparison of the geostrophic and ageostrophic winds in Figs. 12 through 16

indicates, at least qualitatively, that there is a regularity in the distribution of the ageostrophic winds in the vicinity of the jet and in the time changes of the ageostrophic wind. Vector deviations to the south of the zone of maximum wind at 12 CST and 18 CST 16 May are strongly towards the west --- roughly at right angles to the flow. While the magnitudes of the deviations appear to be too large to be purely the result of friction at this level, they can be explained at least partially through the convective acceleration of the air as it moves into the isotach maximum. At 00 CST, the ageostrophic wind vectors have rotated to the right, now pointing to the northwest or north over much of the area, with a sizeable component in the direction of the motion. This is precisely the type of rotation described by Blackadar. Changes in the ageostrophic wind thereafter do not appear to fit this simple model. This could perhaps be explained by changes in the geostrophic winds and in the convective acceleration terms (see equation 2), both of which have been assumed by Blackadar to be negligible; however, the topic did not seem worth pursuing with this particular data unless a more accurate calculation could be made of the ageostrophic wind and its time derivative.

## 5. Estimation of the Thermal Wind Within the First Kilometer

In Fig. 21, the vertical shears of the ageostrophic winds within the lowest kilometer appear to be quite small; however, they cannot be ignored in a direct comparison of the geostrophic and ageostrophic winds at the level of the jet. Several attempts were made to define this shear at each of the observation times in order to pursue the discussion of the ageostrophic wind; however, no method could be found for estimating the thermal wind with sufficient accuracy from the available temperature data.

The method described in the previous section (the analysis of mean virtual temperatures from upper air data) proved to be unsatisfactory for several reasons:

1. Because of the sloping terrain, estimates of the gradient of the mean virtual temperature along a constant pressure surface must be computed from a series of charts with varying horizontal dimensions. For

instance, the 950 mb surface intersects the ground at 99 to 100 deg W. Thus, estimates of the temperature gradient within the layer from 900 to 950 mb must be based upon observations from only a few stations, in the central and eastern section of the region. Near the ground, mean temperatures are strongly dependent upon the lapse rate within the lowest few hundred meters. It was difficult to define the larger scale temperature fields since these lapse rates are influenced by local conditions of cloud cover, topography and wind. In the cases presented in Fig. 24, thermal wind shears within the lowest 50 mb were determined primarily by a downward extrapolation of the temperature patterns at higher levels.

2. Since temperature soundings aloft are available only at 18 CST and 06 CST, it is necessary to assume some sort of regular change in the temperature fields in order to estimate the thermal winds at the other observation times. Simple advection of the isotherms or linear interpolation of the positions of particular isotherms did not seem legitimate since the most pronounced temperature changes near the ground are the result of the heat lost or gained through radiation.

Considerable time and effort was spent in trying to analyze and extrapolate the thermal wind fields aloft before this approach was abandoned. A second attempt was made using the surface temperature data.

Smoothed isotherms were drawn at the surface at each of the five observation times. Estimates were made of the horizontal gradient of the temperature at the level of the terrain under the assumption that this should be closely related to the mean horizontal temperature gradient within the lowest kilometer.

The thermal wind equations were written in the following approximate form:

$$\frac{\partial u}{\partial z} = -\frac{g}{fT}\frac{\partial T}{\partial y} \qquad \frac{\partial v}{\partial z} = \frac{g}{fT}\frac{\partial T}{\partial x} \tag{3}$$

(see, for example, Hess, 1959). Symbols have their usual meaning.

The temperature derivative $\partial T/\partial x$ , for example, may be written

$$\frac{\partial T}{\partial x} = \frac{\delta T}{\delta x} - \frac{\partial T}{\partial z}\frac{\delta z}{\delta x} ,$$

where the differentials denoted by $\delta$ refer to increments measured along the sloping terrain. A similar expression may be written for the y derivative of temperature. Thus, equations (3) may be written

$$\begin{aligned} \frac{\partial u}{\partial z} &= -\frac{g}{fT}\frac{\delta T}{\delta y} + \frac{g}{fT}\left(\frac{\partial T}{\partial z}\right)\frac{\delta z}{\delta y} \\ \frac{\partial v}{\partial z} &= \frac{g}{fT}\frac{\delta T}{\delta x} - \frac{g}{fT}\left(\frac{\partial T}{\partial z}\right)\frac{\delta z}{\delta x} \end{aligned} \qquad (4)$$

The terms in equations (4) involving the slope of the terrain cannot be ignored. Their contribution to the thermal wind within the lowest kilometer in western Kansas and Oklahoma is as large as 10 m sec $^{-1}$ .

The terrain slope ($\delta z/\delta x$, $\delta z/\delta y$) was computed at grid points over the entire area using the mean-terrain map constructed by McClaine (1960). During the day, lapse rates were assumed to be nearly dry adiabatic over most of the region and at night, approximately isothermal.

The results of this experiment, however, were not satisfactory. At 18 CST and 06 CST, the winds obtained by building upward from the surface were, in general, 20 deg or more to the right of the most likely direction of the geostrophic flow at 850 mb. While this does not seem to be a large error, with winds of 20 m sec $^{-1}$ the error corresponds to an uncertainty in the ageostrophic wind of the order of 8 m sec $^{-1}$ .

## 6. Summary and Conclusions

Attempts to measure the ageostrophic winds in the vicinity of the low-level jet stream were not successful; however, several features of the observed and geostrophic winds are worth noting;

1. The low-level jet stream on quasi-horizontal charts is not a reflection of the geostrophic wind. Geostrophic wind speeds were roughly uniform throughout the region of southerly flow yet a distinct isotach maximum was apparent on the quasi-horizontal charts. The low-level jet

stream must be viewed as a superposition of a strong ageostrophic wind field within this broad region of roughly uniform geostrophic glow.

2. Wind maxima are completely ageostrophic in the vertical. Thermal wind shears at Tulsa, Oklahoma City and Fort Worth gave no indication of a vertical maximum in the geostrophic wind.
3. While the low-level jet stream did exist during the daytime, it was much more cohesive and more pronounced during the night-time hours. The night time increase in speeds takes place roughly as described by Blackadar (1957), as a fairly uniform acceleration of the wind within the entire region of southerly flow.

The experiment with the isallobaric wind must be regarded as a failure. The geostrophic wind has been shown to be a valid approximation to the actual wind in certain cases and for certain scales of atmospheric motions (Charney, 1948). It has not been demonstrated that the isallobaric correction (eq. 1) gives a useful approximation for any scale of motion. It is obviously unrealistic in the mesoscale where pressure tendencies may be practically discontinuous. Inclusion of the isallobaric term did not give a useful approximation to the actual wind in the case examined here and studies by Haurwitz (1946) and by Houghton and Austin (1946) have failed to indicate any validity to the isallobaric winds as determined from 12-hour pressure changes at 10000 feet. It would seem that the burden of proof is, at this point, entirely upon the isallobaric wind.

A fundamental problem in analysis of the type presented here is the difficulty in attempting to define two scales of motion from two different network densities. A surface pressure analysis can be made quite accurately with the NSSP data; the elimination of the meso-systems constituted a real problem only in determining the pressure tendencies. However, until a much more complete network of wind and temperature observations can be established aloft, attempts to combine the surface NSSP data with the data at higher levels will probably always be unsatisfactory.

## References


Blackadar, A. K., 1957: Boundary layer wind maxima and their significance for the growth of nocturnal inversions. Bull. Amer. Meteor. Soc., 38, 283-290.

Bonner, W. D., 1963: Thunderstorms and the low-level jet. Mesomet. Res. Paper 22, Univ. of Chicago.

Brunt, D. and C.K.M. Douglas, 1928: The modification of the strophic balance for changing pressure disturibution, and its effect on rainfall. Mem. Roy. Meteor. Soc., 3, 29-51.

Charney, J.G., 1948: On the scale of atmospheric motions. Geophys. Publ., 17, No. 2, 1-17.

Fujita, T., 1962: A review of Researches on analytical mesometeorology. Mesomet Res. Paper 8, Univ. of Chicago.

----------and H.A. Brown, 1957: A revised method of pressure reduction. Tech. Rept. 4, Univ. of Chicago.

Haltiner, G. and F. Martin, 1957: Dynamical and Physical Meteorology. New York, McGraw-Hill, 470pp.

Haurwitz, B., 1946: On the relation between the wind field and pressure changes. J. Metero., 3, 95-99.

Hess, S. L., 1959: Introduction to Theoretical Meteorology. New York, Henry Holt and Company, 362pp.

Houghton, H.G. and J. M. Austin, 1946: A study of non-geostrophic flow with applications to the mechanism of pressure changes. J. Meteor., 3, 57-77.

McClaine, E. P., 1960: Some effects of the western cordillera of North America on cyclone activity. J. Meteor., 17, 105-115.

Means, L. L., 1962: Comments on "The low-level jet as related to nocturnal thunderstorms over midwest United States." J. Appl. Meteor., 1, No. 4, p. 588.

Newton, C.W., 1956: Mechanisms of circulation change during a lee cyclogenesis. J. Meteor., 13, 528-539.

Petterssen, S., 1956: Weather Analysis and Forecasting. Vol 1, (2nd Ed.), New York, McGraw-Hill, 428pp.

Pitchford, K. L. and J. London, 1962: The low-level jet as related to nocturnal thunderstorms over midwest United States. J. Appl. Meteor., 1, No. 1, 43-47.

Sangster, W., 1959: A meteorological coordinate system in which the earth's surface is a coordinate surface. Scient. Rept. No. 8, Univ. of Chicago.

Wexler, H., 1961: A boundary layer interpretation of the low-level jet. Tellus, 13, No. 3, 368-378.

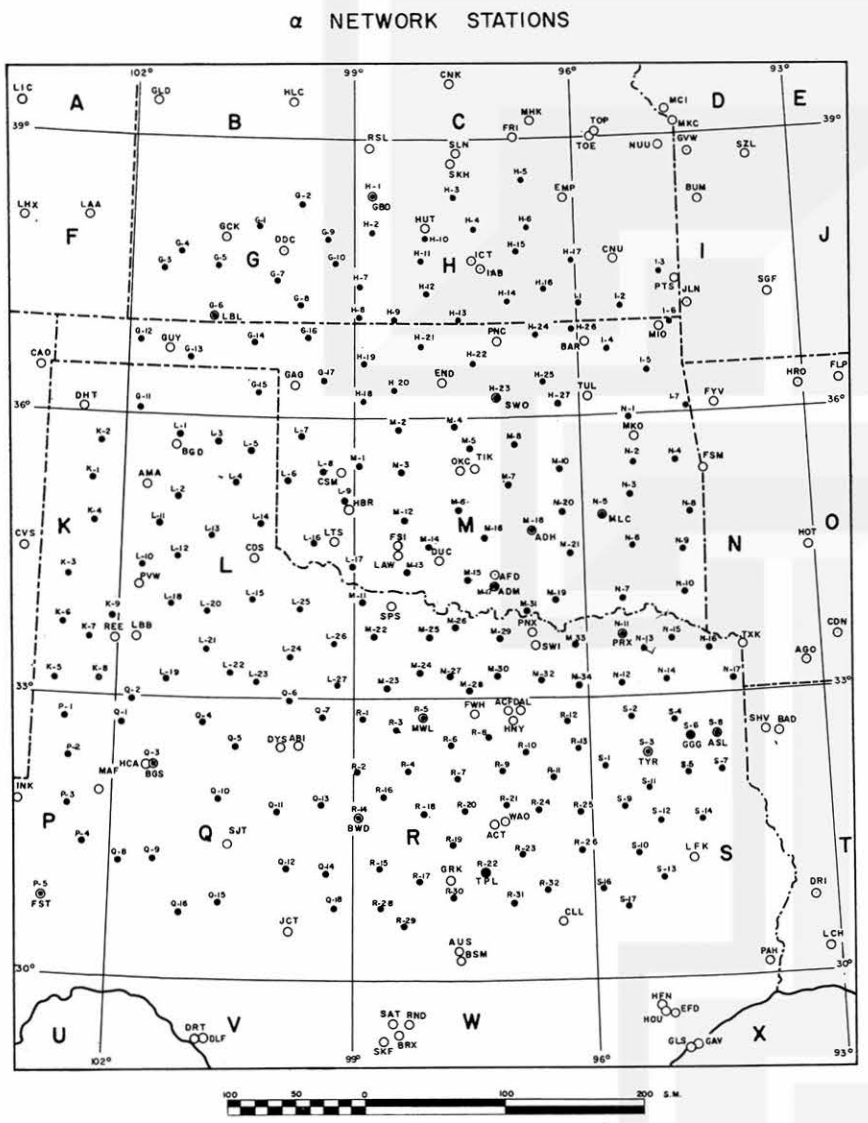


Fig. 1 NSSP area. Alpha network stations indicated by black dots.

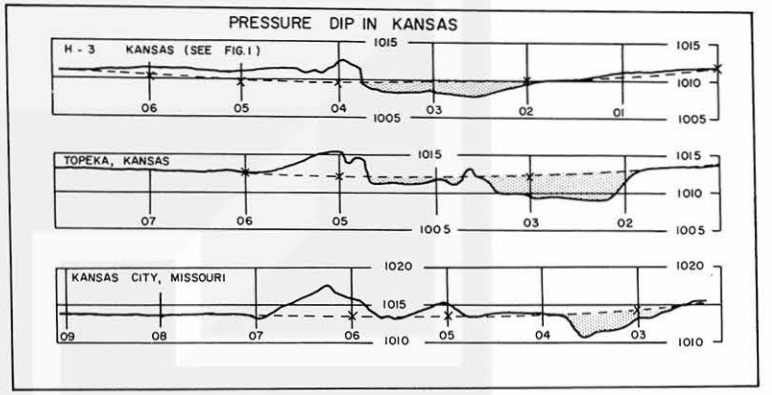


Fig. 2 Pressure traces in the vicinity of an intense squall line in northern Kansas. Synoptic charts during the period are shown in Figs. 3, 4, and 5.

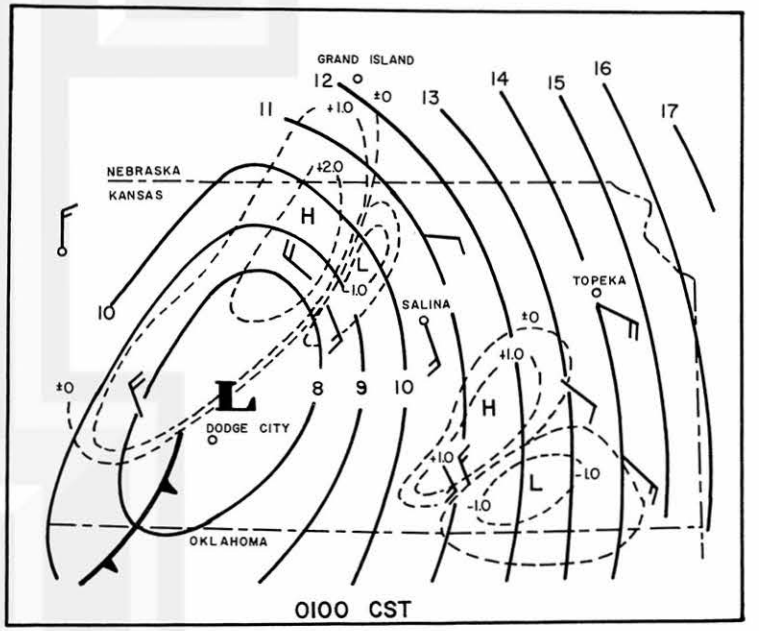


Fig. 3 Smoothed (solid line) and excess (dashed line) pressures associated with the squall line in northern Kansas. Winds are plotted in standard synoptic fashion. Map time is 01 CST.

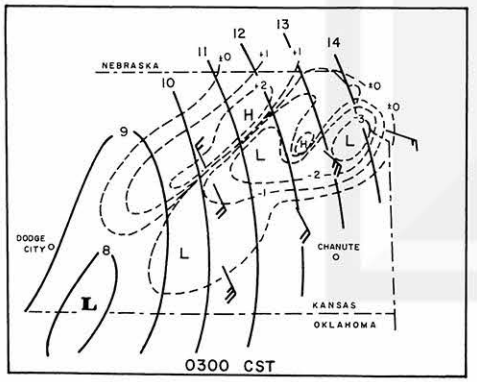


Fig. 4 Same as Fig. 3 except at 03 CST.

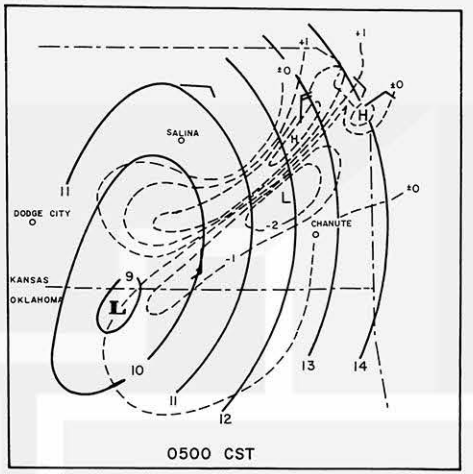


Fig. 5. Same as Fig. 3 except at 05 CST.

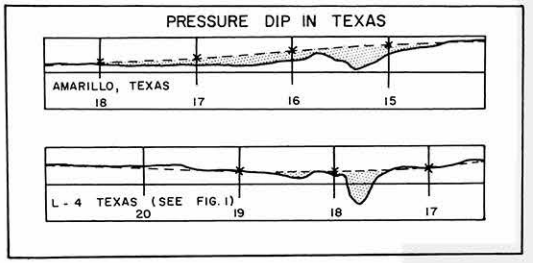


Fig. 6 Pressure traces at Amarillo Texas and alpha station L-4 (see Fig. 1) during the early stages of squall line development.

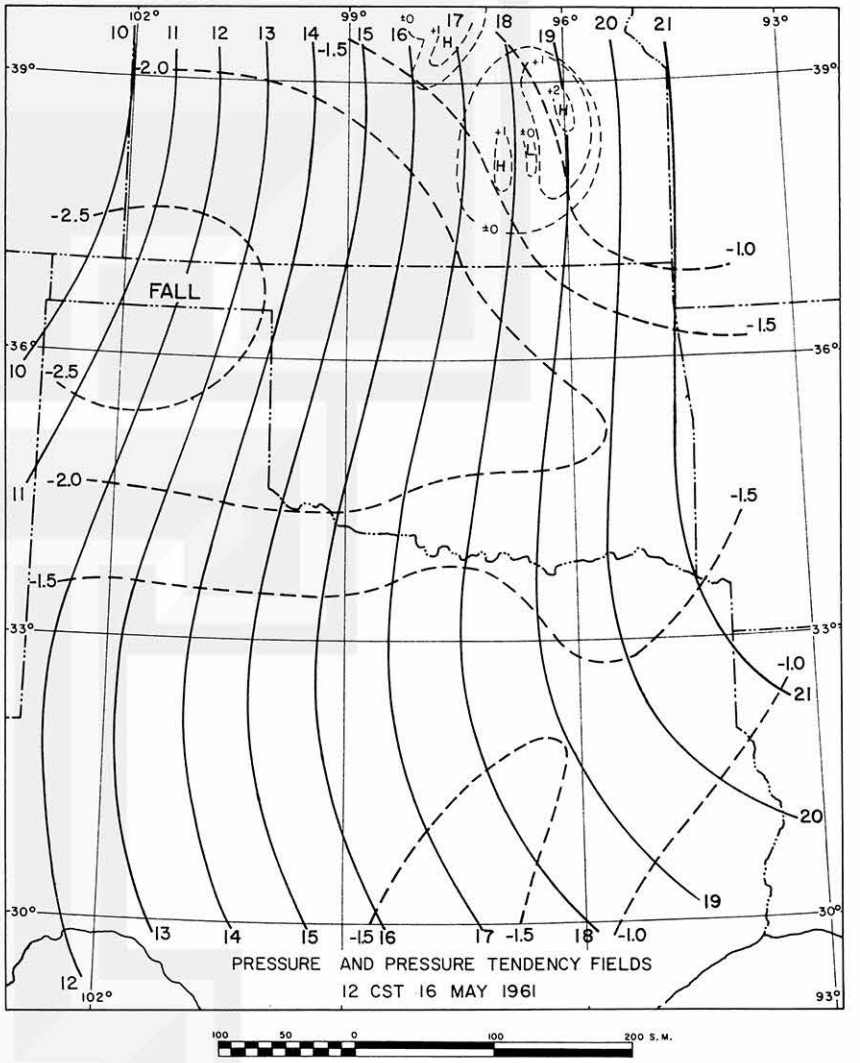


Fig. 7 Smoothed pressures, excess pressures and pressure tendency fields as determined from the NSSP data. The excess pressures associated with the mesosystems are indicated by light dashed lines; isallobars by heavy dashed lines. Map time is 12 CST, 16 May, 1961.

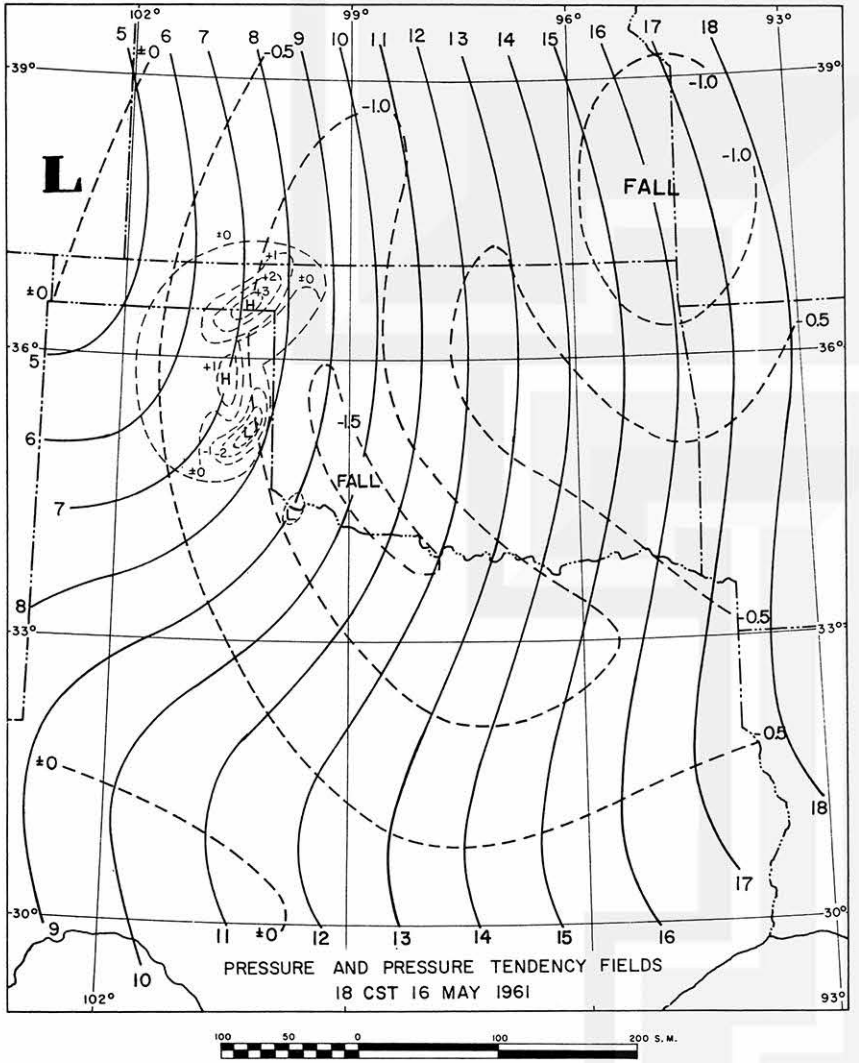


Fig. 8 Same as Fig. 7 except at 18 CST, 16 May.

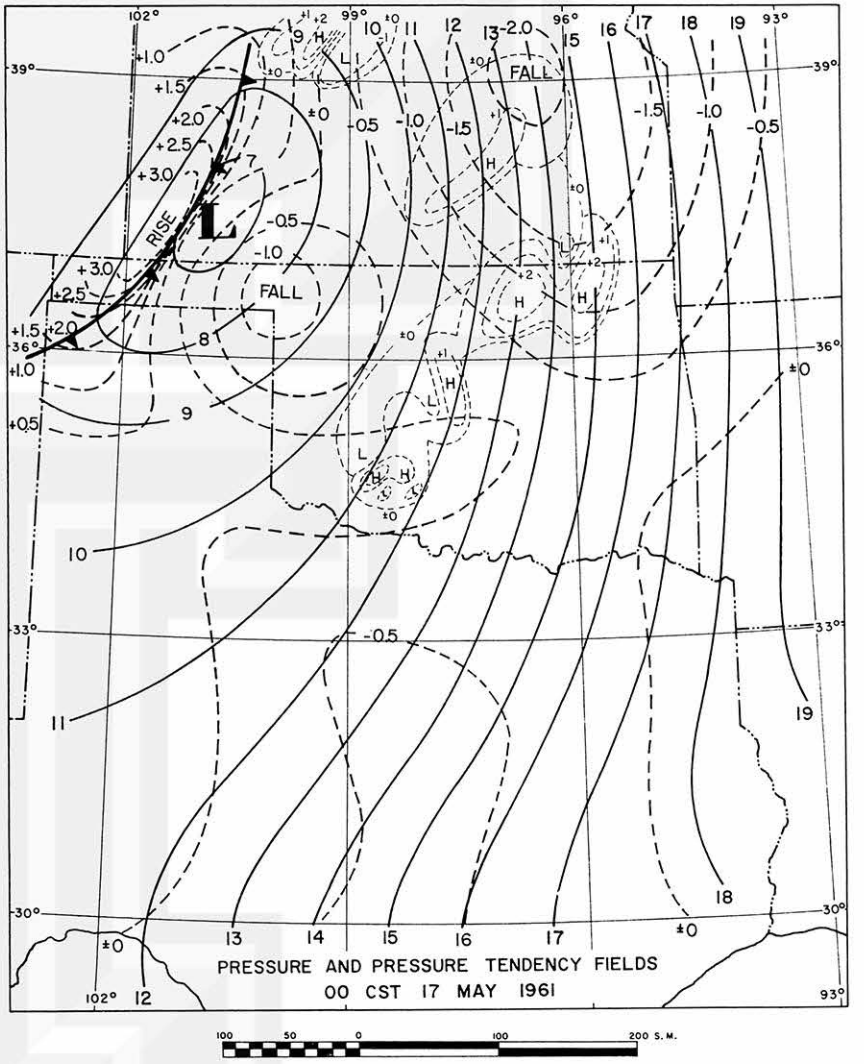


Fig. 9 Same as Fig. 7 except at 00 CST, 17 May.

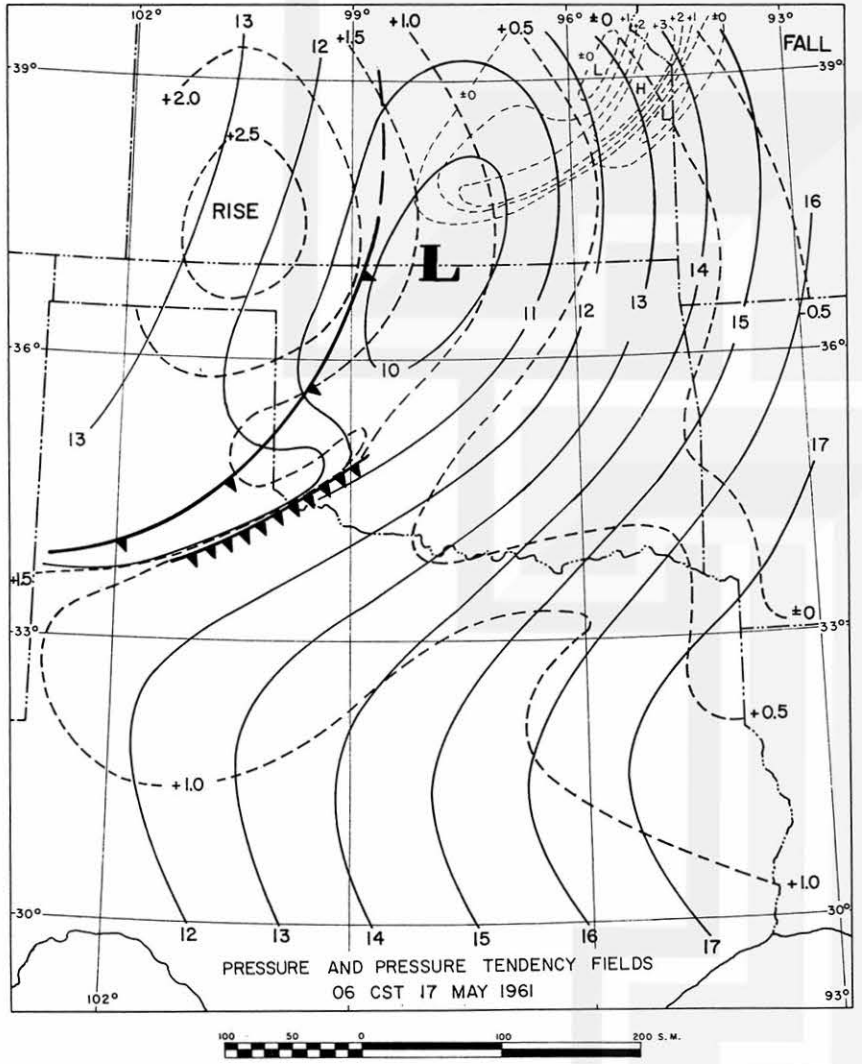


Fig. 10 Same as Fig. 7 except at 06 CST, 17 May.

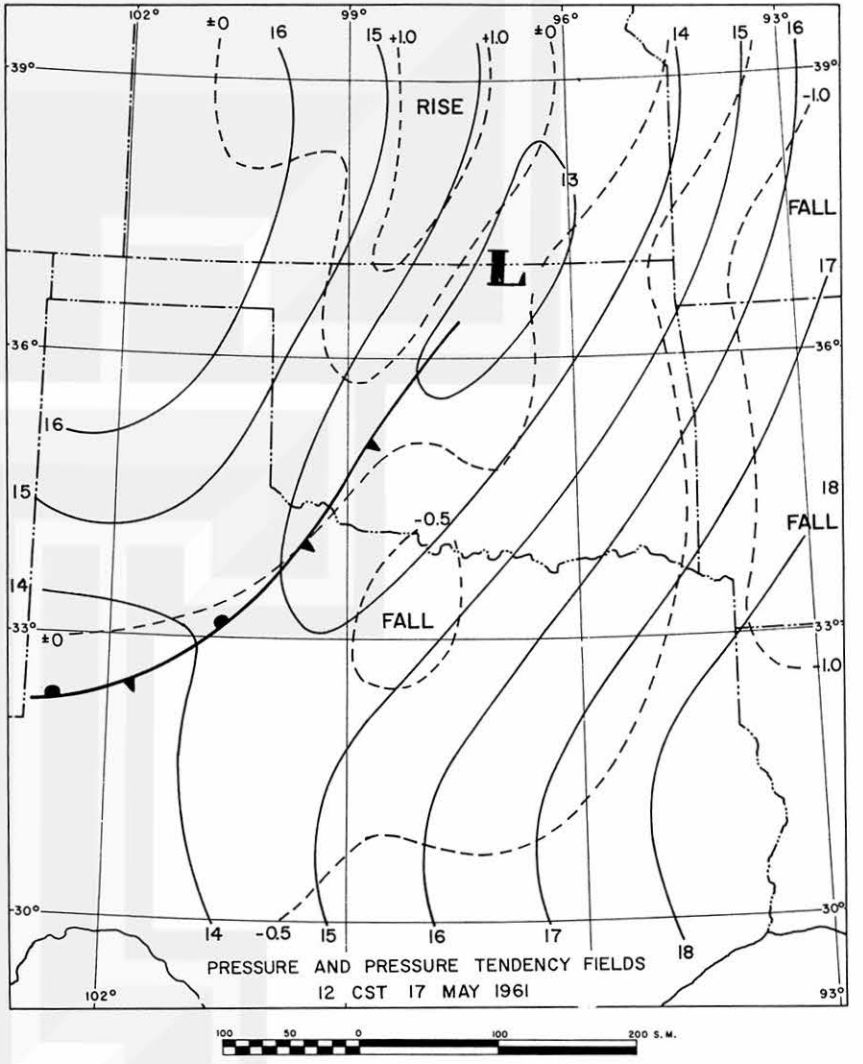


Fig. 11 Same as Fig. 7 except at 12 CST, 17 May.

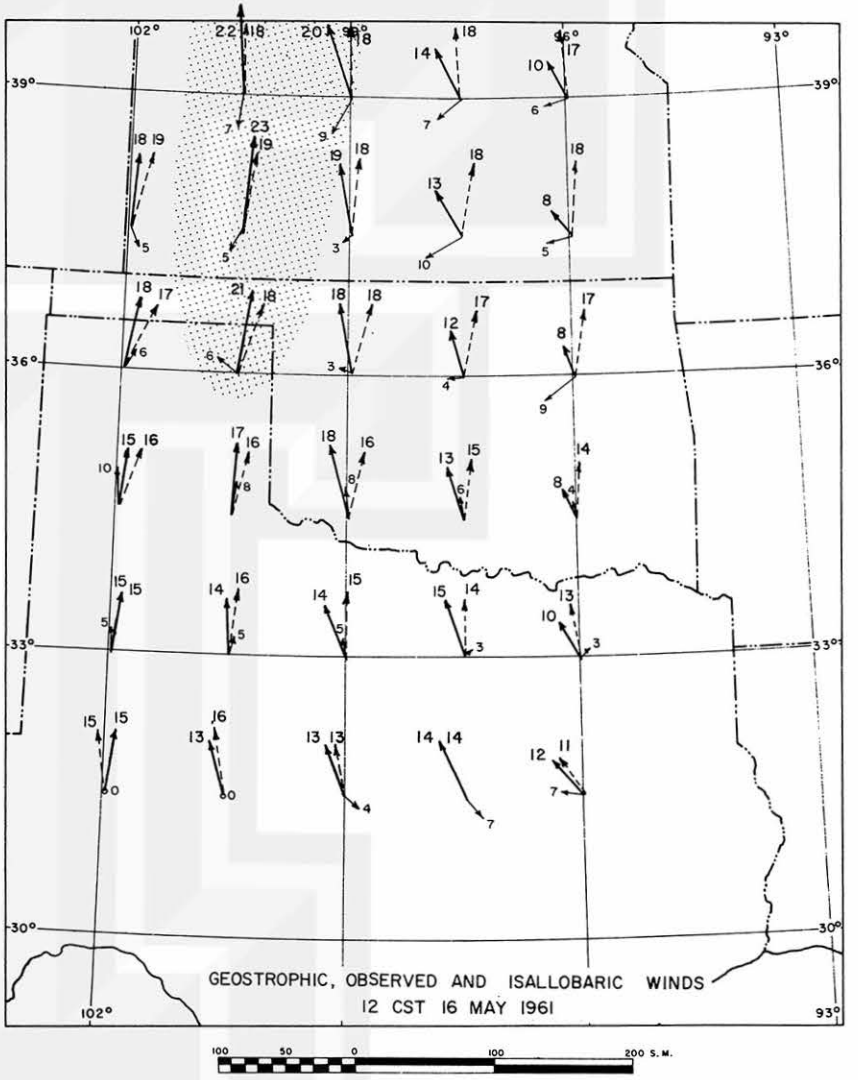


Fig. 12 Geostrophic and isallobaric components of the wind at 12 CST, 16 May. Dashed vector is the geostrophic wind; light solid vector is the isallobaric component of the wind. Observed winds as determined by streamline and isotach analyses at 1 km above the ground are indicated by the heavy vectors. Wind speeds in m $sec^{-1}$ are written by the head of the appropriate vector. Shaded areas denote regions of strongest winds. Light shading indicates speeds between 20 and 25 m $sec^{-1}$; medium (see Fig. 14) 25 to 30 m $sec^{-1}$; heavy, greater than 30 m $sec^{-1}$.

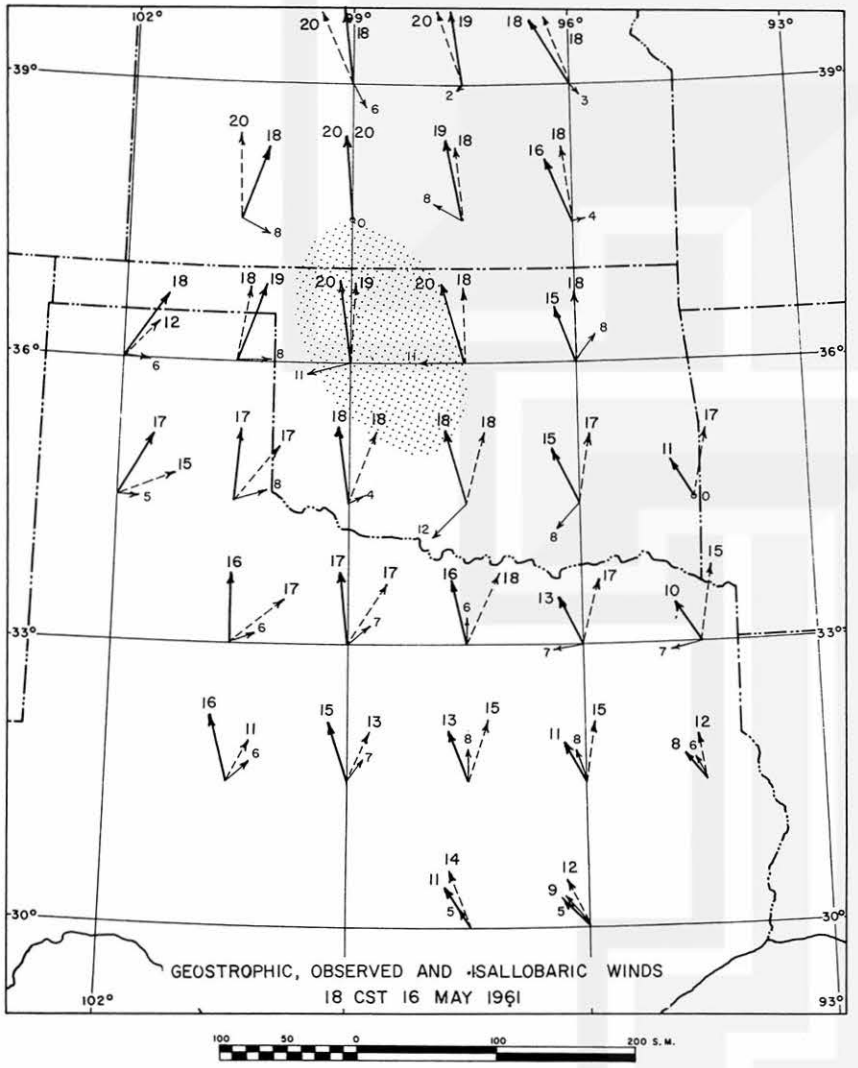


Fig. 13 Same as Fig. 12 except at 18 CST, 16 May.

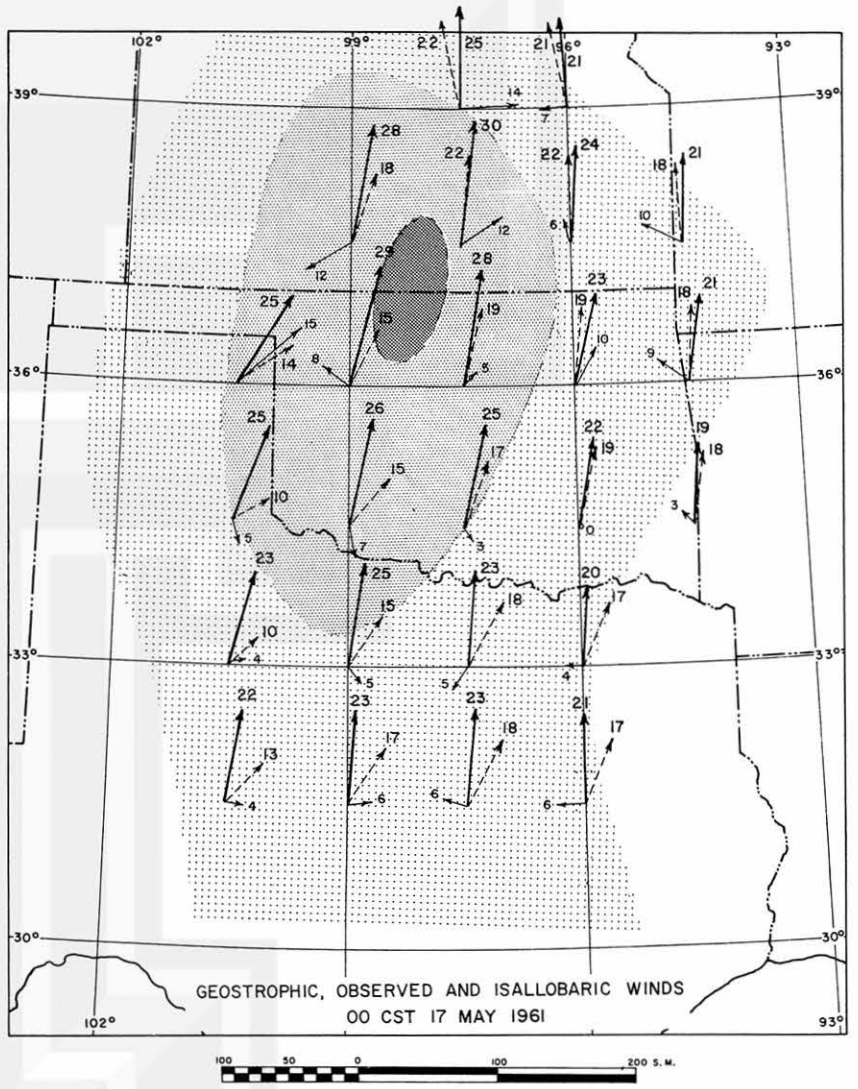


Fig. 14 Same as Fig. 12 except at 00 CST, 17 May.

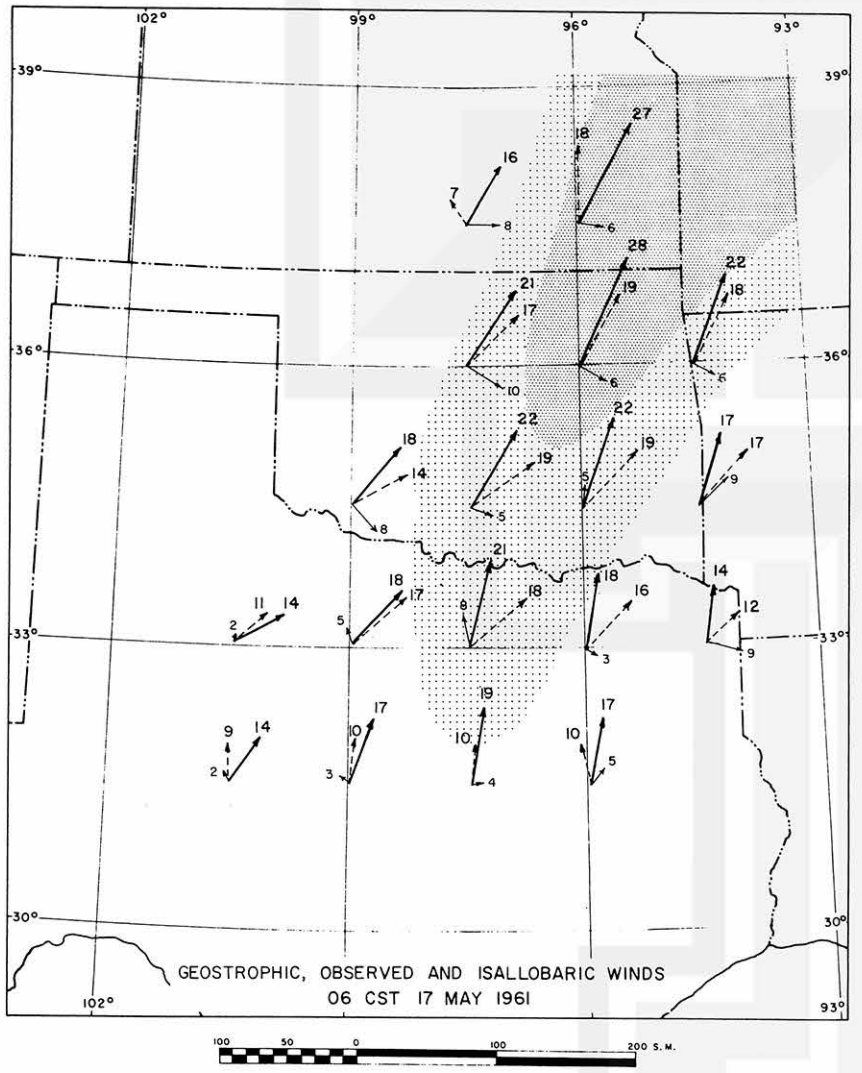


Fig. 15 Same as Fig. 12 except at 06 CST, 17 May.

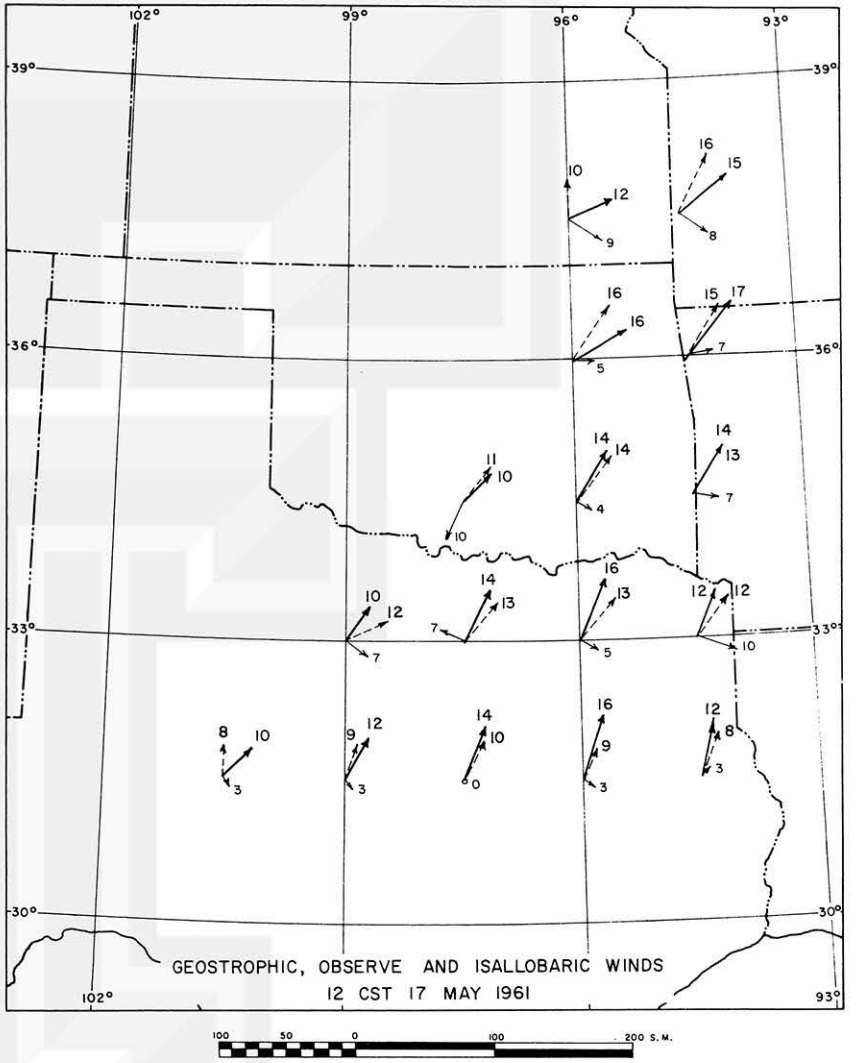


Fig. 16 Same as Fig. 12 except at 12 CST, 17 May.

Fig. 17 Vertical cross-section of the southerly (solid line) and westerly (dashed line) components of the wind at 35 deg N. 18 CST, 16 May, 1961. Heavy, broken line indicates the level of maximum wind in the southerly flow.

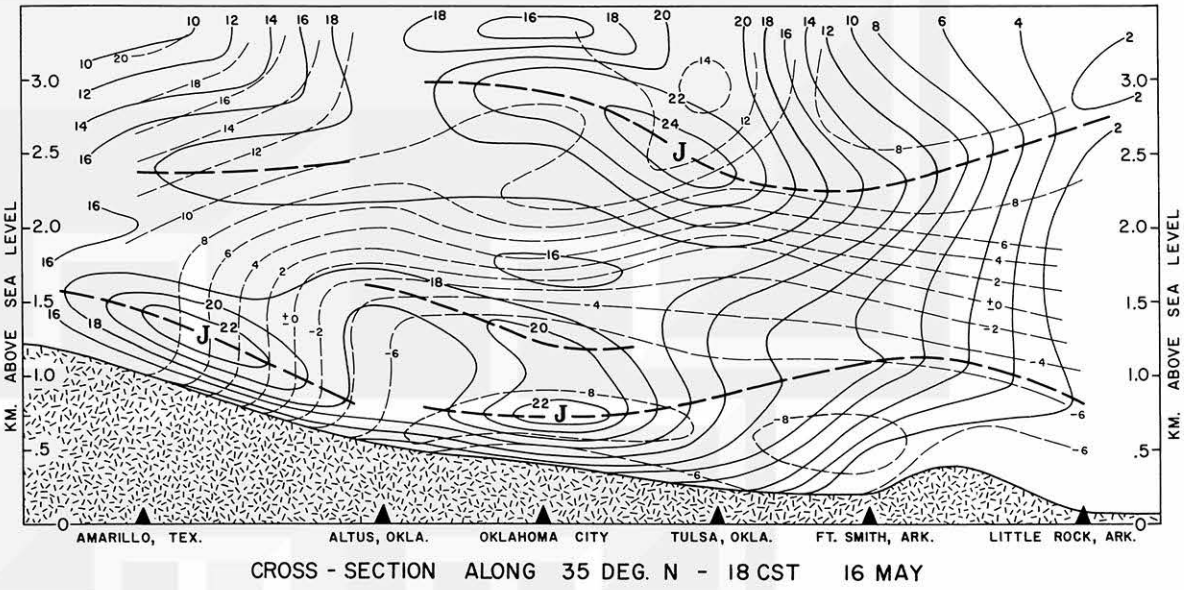


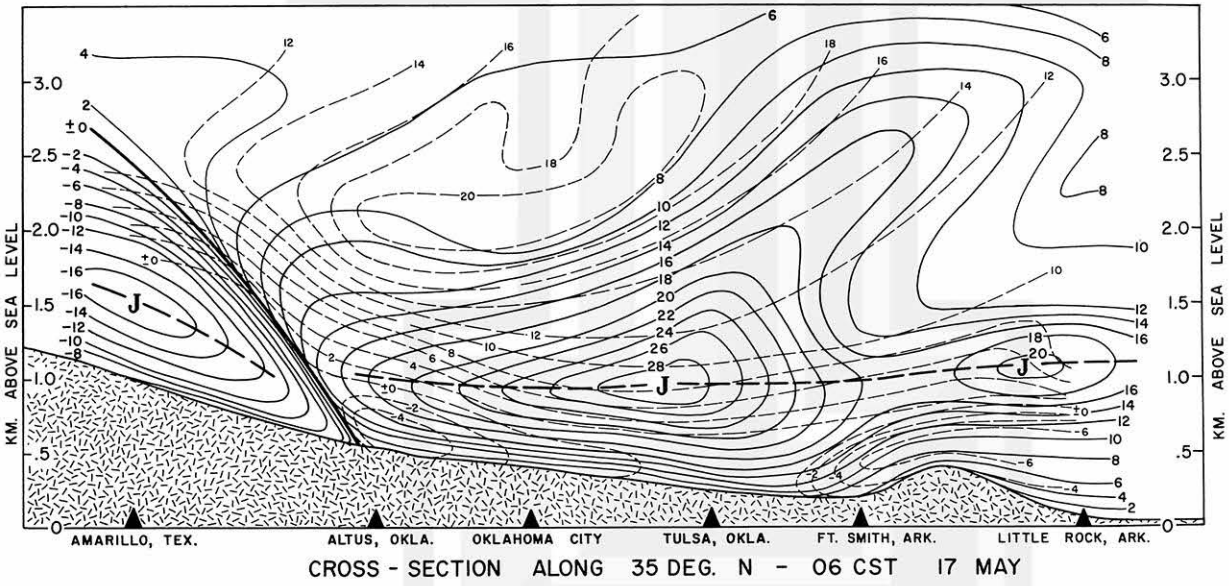


Fig. 18 Same as Fig. 17 except at 06 CST, 17 May, 1961.

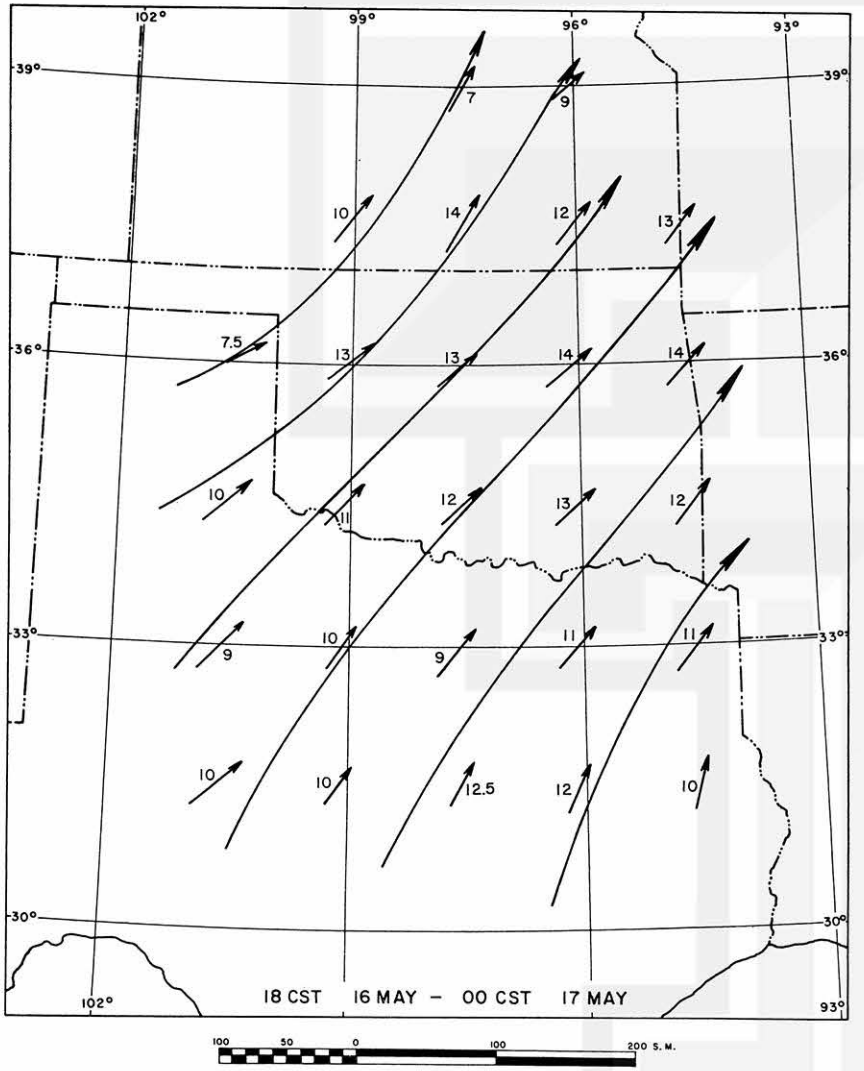


Fig. 19 Six-hour vector-wind changes in m $sec^{-1}$ per 6 hrs. during the period 18 CST, 16 May to 00 CST, 17 May.

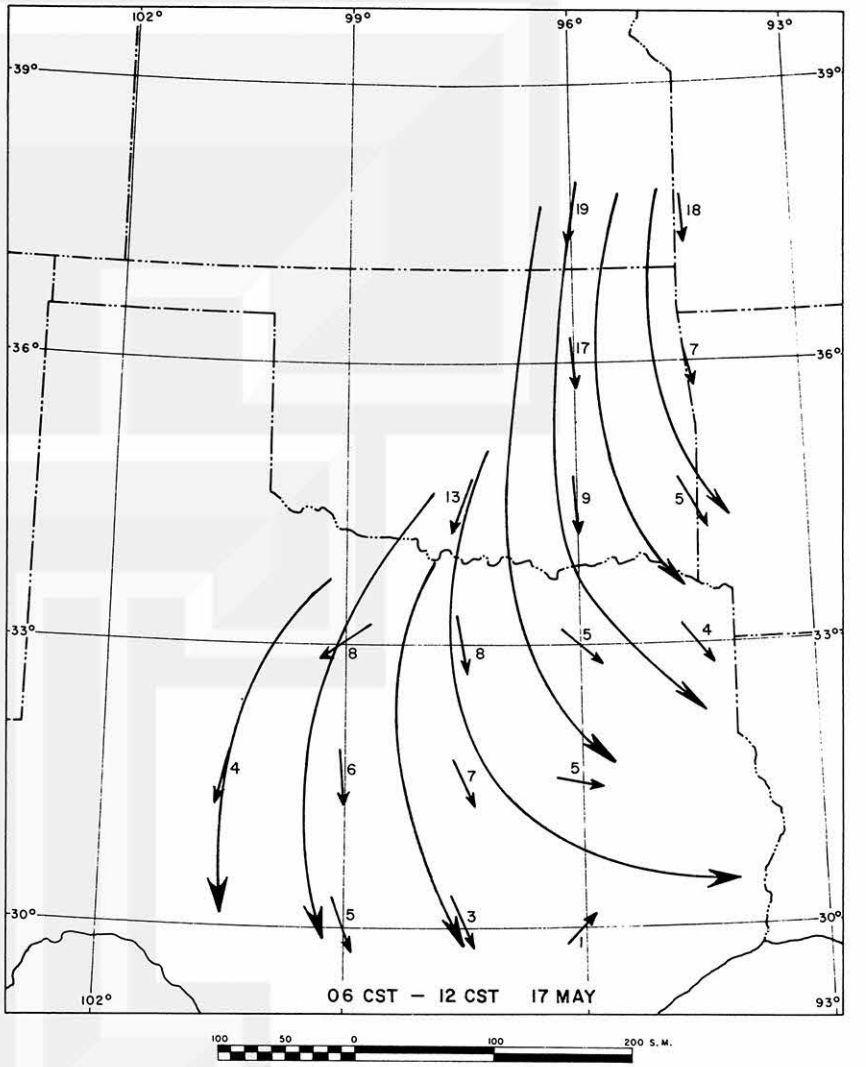


Fig. 20 Six-hour vector-wind changes during the period 06 CST, 17 May to 12 CST, 17 May.

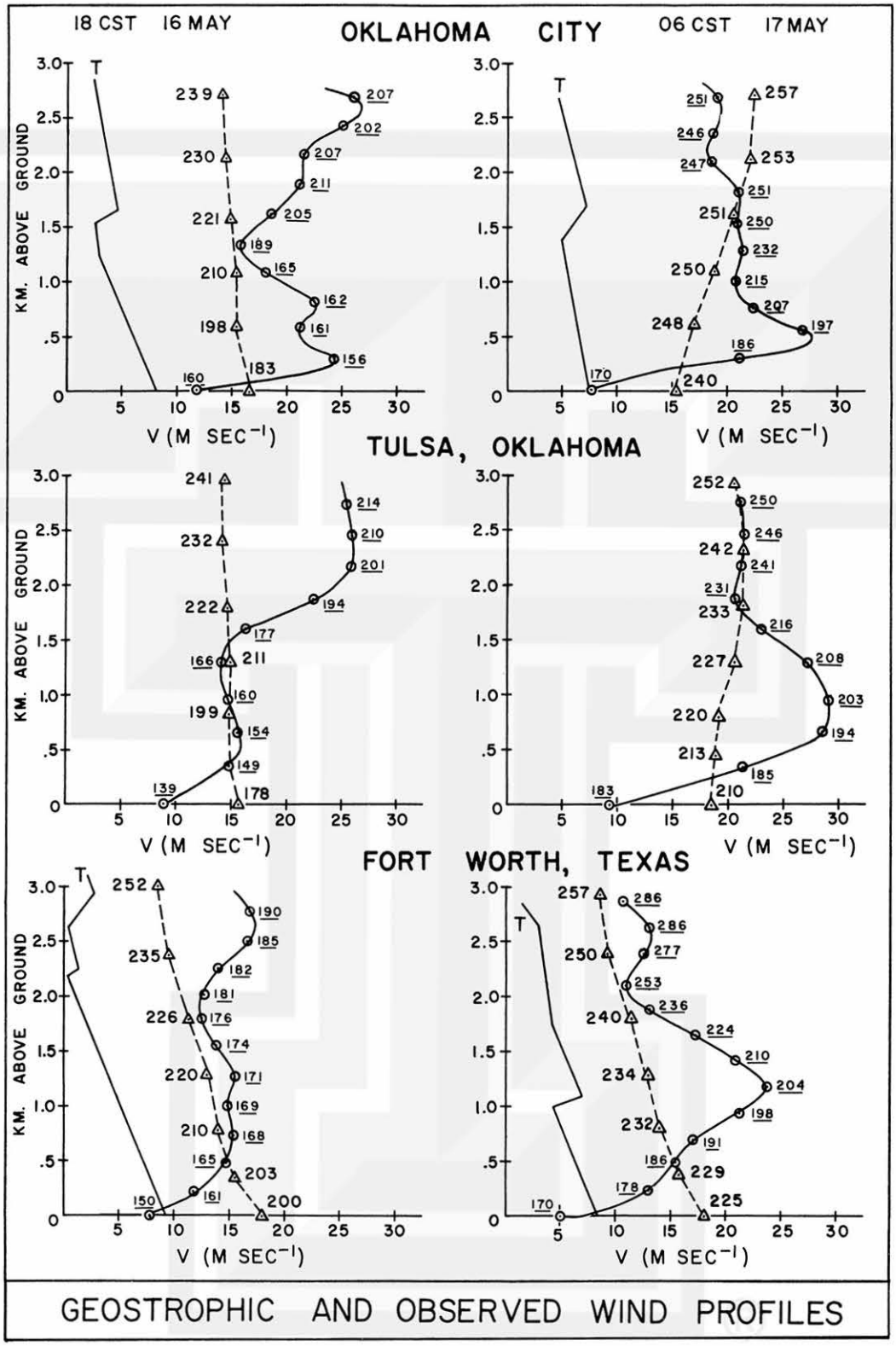


Fig. 21 Vertical profiles of the observed and geostrophic winds from ground level to 700 mb at selected locations. Wind directions are given at the various levels. Solid lines and small, underlined wind directions refer to the actual wind. Temperature profiles are given schematically where radiosonde observations were available.

MESOMETEOROLOGY PROJECT ------- RESEARCH PAPERS

(Continued from front cover)

16. Preliminary Result of Analysis of the Cumulonimbus Cloud of April 21, 1961 - Tetsuya Fujita and James Arnold

17. A Technique for Precise Analysis of Satellite Photographs - Tetsuya Fujita

18. Evaluation of Limb Darkening From TIROS III Radiation Data - S.H.H. Larsen, Tetsuya Fujita, and W. L. Fletcher

19. Synoptic Interpretation of TIROS III Measurements of Infrared Radiation - Finn Pedersen and Tetsuya Fujita

20. TIROS III Measurements of Terrestrial Radiation and Reflected and Scattered Solar Radiation - S.H.H. Larsen, T. Fujita, and W.L. Fletcher

21. On the Low-level Structure of a Squall Line - Henry A. Brown

22. Thunderstorms and the Low-level Jet - William D. Bonner

23. The Mesoanalysis of an Organized Convective System - Henry A. Brown

24. Preliminary Radar and Photogrammetric Study of the Illinois Tornadoes of April 17 and 22, 1963 - Joseph L. Goldman and Tetsuya Fujita

25. Use of TIROS Pictures for Studies of the Internal Structure of Tropical Storms - Tetsuya Fujita with Rectified Pictures from TIROS I Orbit 125, R/O 128 - Toshimitsu Ushijima